Bull Eng Geol Environ
DOI 10.1007/s10064-013-0542-z

ORIGINAL PAPER

Time-dependent damage constitutive model for the marble in the Jinping II hydropower station in China

Bing-Rui Chen · Xiao-Jun Zhao · Xia-Ting Feng · Hong-Bo Zhao · Shan-Yong Wang

Received: 22 February 2013 / Accepted: 17 October 2013

Abstract To accurately describe the damage creep properties of marble, especially during the acceleration creep phase, creep testing was performed on the marble in the Jinping II hydropower station in China. Based on the experimental results, a time-dependent damage constitutive model was proposed in terms of fractional calculus theory and damage variables to describe these time-dependent damage characteristics. The time-dependent constitutive equations were derived for constant loading levels below and above the marble's long-term strength. The robustness and parameter sensitivity of the proposed model were analysed by utilizing data of creep testing. The results of the analysis showed that the proposed model could describe not only the attenuation and steady-state creep of marble but also the acceleration creep characteristics and negative exponential attenuation law of the yield strength over time when the constant loading was above the long-term strength. These are crucial to failure prevention during rock engineering construction and operating periods.

Keywords Creep testing · Time dependent damage characteristics · Yield strength · Constitutive model · Fractional calculus theory

Introduction

Rock is a complex heterogeneous natural geological material containing cracks, joints and various defects that give it a wide range of different time-dependent characteristics and constitutive relationships (Chen and Feng 2008). Many time-dependent constitutive models of rocks have been proposed by researchers in the past decades (Jin and Cristescu 1998; Deng 2001; Zhou 2011; Wang 2004). Traditional time-dependent constitutive models (such as the generalised Kelvin model, Burgers model, Nishihara model and a combination of the spring, dashpot and Saint–Venant body model) are unable to accurately reflect the rock's accelerated creep characteristics (You 2007). In order to describe the time-dependent characteristics of rock masses in the acceleration creep stage, Jin and Cristescu (1998) suggested a new elastic/viscoplastic transient creep model based on triaxial experimental data of Gorleben salt rock. Deng in (2001) considered the stress of viscous dampers to be proportional to their creep acceleration and combined a modified Bingham body with a Cunshan body to describe nonlinear visco-plastic evolution characteristics over time in the accelerated creep phase. Xu (2005) assumed that strain is proportional to the n power of time (where n is the creep index reflecting the rock's accelerated creep velocity) and established a nonlinear time-dependent model to describe rock's accelerated creep characteristic utilising a nonlinear time-dependent component instead of the conventional linear time-dependent component. Zhou (2011) proposed a new

B.-R. Chen (✉) · X.-T. Feng
State Key Laboratory of Geomechanics and Geotechnical Engineering, Institute of Rock and Soil Mechanics, Chinese Academy of Sciences, 2# Xiaohongshan, Bayi Road, Wuhan 430071, Hubei, China
e-mail: brchen@whrsm.ac.cn

X.-J. Zhao · H.-B. Zhao
School of Civil Engineering, Henan Polytechnic University, Jiaozuo 454003, Henan, China

S.-Y. Wang
ARC Centre of Excellence for Geotechnical Science and Engineering, Department of Civil, Surveying and Environmental Engineering, The University of Newcastle Callaghan, Newcastle, NSW 2308, Australia

Published online: 19 November 2013

creep constitutive model on the basis of a time-based fractional derivative by replacing a Newtonian dashpot in the classical Nishihara model with the fractional derivative Abel dashpot. By introducing the concept of a damage accelerating limit to the Carter creep model, Wang (2004) presented a new constitutive creep-damage model to describe the tertiary creep of salt rock. Molladavoodi and Mortazavi (2011) proposed a damage-based numerical analysis method for describing brittle rock failure mechanisms. Xie (2011) presented a micromechanics-based elastoplastic damage model for quasi-brittle rocks under a compressive stress state with a proposed coulomb-type friction criterion based on the strain energy release rate.

Although there have been many endeavours to investigate and construct a time-dependent damage constitutive model that can describe the time-dependent damage characteristics of rock masses and solve the time-dependent mechanics problems encountered in rock mechanics and engineering, the time-dependent damage characteristics and yield strength's time-dependent evolution law of deeply buried hard rock always are investigated separately. It is not enough to accurately describe time-dependent damage characteristics of rock material and further investigations are required. Bagley and Torvik (1983) deemed that fractional calculus time-dependent constitutive models had much better advantages for describing the material's visco-elastic mechanical properties than integer-order calculus. These constitutive models have been widely used on polymer materials in recent years (Koeller 1984; Song and Jiang 1998; Welch et al. 1999; Beda and Chevalier 2004).

In the present study, a constitutive model to describe the time-dependent damage characteristics of the Marble in the Jinping II Hydropower Station in China is proposed. Firstly, laboratory tests are carried out to investigate the time-dependent evolutionary law of Jinping's marble damage characteristics and rock yield strength under long-term loading. Furthermore, fractional calculus theory to describe the rock material's visco-elastic behaviour is introduced. Moreover, damage variables to describe the degradation phenomena of rock's mechanical parameters over time are introduced. Finally, a time-dependent constitutive model that accurately describes changes to the damage properties and yield strength of the marble over time is established.

Time-dependent failure characteristic of Jinping marble in situ

The Jinping II hydropower station is located on the Great Jinping River Bend of Yalong River in Jinping, Liangshan Yi Autonomous Prefecture, Sichuan of China. It takes advantage of an about 310 m natural drop in the river at the bend and diverts the water to headrace tunnels travelling through Jinping Mountain (see Fig. 1a). There are seven parallel tunnels and the length of each tunnel is approximately 16.7 km. A total of 75.8 % of the tunnel lengths are covered by over 1500 m of rock mass and the maximum depth of the tunnels is approximately 2,525 m. Feng and Zhou (2006) deemed that the tunnels' stress fields changed from the local stress of the river valley to a gravitational stress field when the depth of rock mass was greater than 1,500 m, where the maximum principal stress was 63 MPa. These deepest areas fell within a high ground stress zone, with a erious potential for damage.

Based on the monitoring for four headrace tunnels and a construction drainage tunnel covered with 1,900–2,500 m of rock mass (stake K5 + 500–K6 + 168 m and stake K7 + 374–K9 + 100 m), a total of 195 rock bursts were recorded during the station's the construction process from October 2010 to September 2011. In the meantime, eighty-nine of these rock bursts, or 54.36 %, occurred outside 24 h of excavation. The longest period between an excavation and a rock burst was 163 days and the maximum distance for a rock burst occurring from the tunnel face was 384 m. Time-dependent failure characteristics of Jinping marble were obvious, as illustrated in Fig. 2.

Time-dependent mechanical testing on Jinping II marble

Although a great deal of time-dependent failure has been observed in situ in the Jinping II hydropower station, further experimental tests are required to reveal the mechanical properties of the marble over time.

Rock samples

Rock samples were taken from testing tunnel No. 2 in Auxiliary tunnel A at Jinping II; the location of which is shown in Fig. 1b and c. This portion of the tunnel was covered with 2,500 m of rock mass that belongs to the grey-white, medium-fine crystalline marbles of the Baishan Group (T2b). The rock was hard and brittle with strong densification. This marble's elasticity modulus varied from 25 to 40 GPa and its deformation modulus was 8–16 GPa. No palpable infilling materials, filling belt or structural plane could be observed in the rock samples with the naked eye. Homogeneous lithology showed that the rock was composed mainly of quartz, potash feldspar, calcite, mica, chlorite and smectite. Processing of the sample is described as follows:

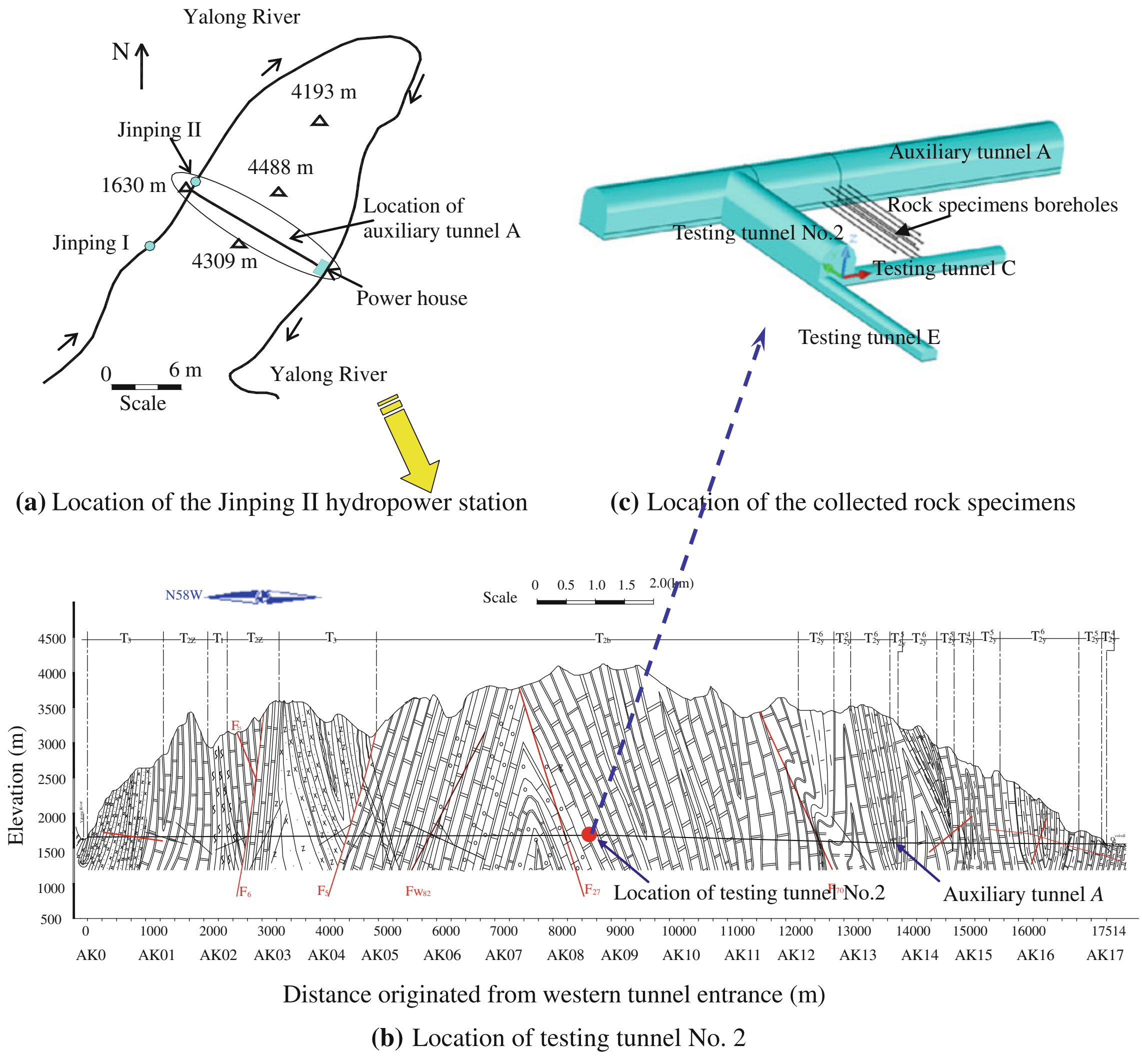

Fig. 1 Location of the collected rock specimens for time-dependent mechanics testing

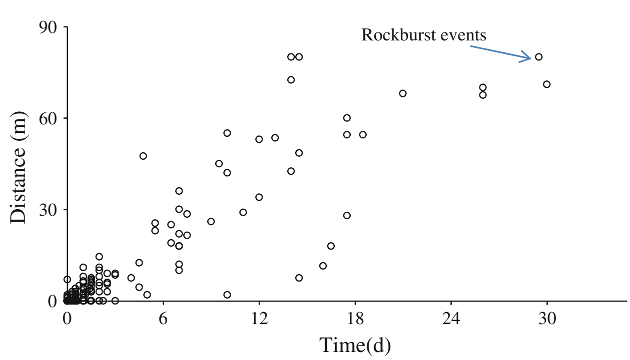

Fig. 2 Spatial and temporal distribution laws of rock burst as headrace tunnels covered in marble were excavated at the Jinping II hydropower station. The *x*-axis shows the time interval between the rock burst zone excavation and the occurrence of rock bursts and the *y*-axis indicates the distance from the tunnel face

1. Firstly, surrounding rockmass was drilled with a drill of diameter of 110 mm in testing tunnel No. 2 and core samples were taken out of boreholes;
2. Then, core samples were immediately covered by protective film to prevent moisture from running out and were put into the special wooden box to avoid being damaged during transportation from the field to the laboratory;
3. In the laboratory, core samples were processed into cylindrical rock samples with a diameter of 50 mm and height of 100 mm. The two end faces of the rock samples were polished smooth, as shown in Fig. 3. The rock samples processing accuracy was strictly controlled in accordance with the Code for Rock Tests of Hydroelectric and Water Conservancy Engineering

Fig. 3 Rock samples for time-dependent mechanical testing

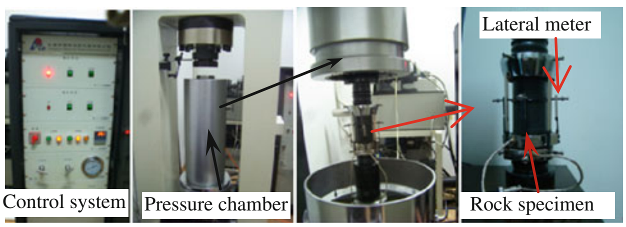

Fig. 4 RC-2000 servo-controlled conventional triaxial rheological testing machine

(Professional Standards Compilation Group of People's Republic of China 2007).

Testing apparatus

Tests were performed with a RC-2000 servo-controlled conventional triaxial rheological testing machine, made by Chaoyang Test Instrument Co., LTD, in China (Fig. 4). The machine's control system adopts the EDC digital servo-controlled device, which is fabricated by DOLI Corporation in Germany. The loading system uses a servo-controlled motor and ball screw system and operates stably. Both axial strain and lateral strain are measured by an extensometer device. The measuring range for axial deformation is 0–8 mm and the lateral deformation measurement ranges from 0 to 5 mm. The measurement error is controlled within ± 1 %. The testing machine can apply a maximum axial load of 2000 kN and the normal surrounding pressure can be controlled at 70 MPa.

Testing process

The uniaxial creep tests were conducted in a special laboratory where the temperature and moisture were controlled at 20 ± 0.5 °C and 70 ± 2 %, respectively, to reduce the impact of thermal and moisture factors on the test results. Before the creep test, firstly the physical property (joints, fissure and other faults inside the rock) of rock sample was tested by emitting the elastic-wave and computed tomography and the similar rock samples were selected and divided into six groups by elastic wave velocity and CT value (Chen 2013), as can been seen in Table 1. Secondly, to obtain the conventional compression strength and calculate the loading step number of the creep test, conventional compression tests were done under the same confining pressure. Then creep tests were begun and testing process followed the next steps as in Table 1.

1. Firstly, a rock sample was covered by heat shrink tubing to prevent oil in the pressure chamber from coming into it and the moisture from running out;
2. Then, the axial and lateral displacement meters were installed on the rock sample, as shown in Fig. 4 and the rock sample was put into the pressure chamber;
3. The axial load was applied stepwise, the first-step applied load was set at 0.6 times the uniaxial compressive strength (UCS) of the rocks. A loading rate of 0.1 MPa/s was used at the loading stages. The axial stress was kept constant after the load reached a preset threshold value.
4. The next load stages were applied until the lateral deformation of the rocks was less than 1×10^{-3} mm in 24 h and the imposed load steps measured 20, 10 and 5 MPa.
5. If rock failure did not occur when the fourth load step was applied to the sample, a load step of 5 MPa was imposed until the rocks failed from rheological acceleration. Recording was stopped and the test ended when the rock sample became unstable.

Time-dependent damage characteristics of Jinping marble

The time-dependent mechanical characteristics evolution laws were similar from group 1–5. For demonstrating the time-dependent mechanical characteristic and building a one-dimension time-dependent mechanical model, group 1 was taken as an example in the paper and other results have been shown by Doctor Chen (Chen 2013). The typical result of time-dependent mechanical testing was shown in Figs. 5 and 9. Some important results are provided.

1. The time-dependent characteristics of the marble were clear and the creep process showed obvious transient creep, attenuation creep, steady-state creep and accelerating creep properties under high stress conditions, as shown in Fig. 5.

Table 1 Velocity and CT value of rock samples and multi-step loading creep test scheme

Group	Series no.	Velocity (m/s)	Relative error (%)[a]	CT value	Relative error (%)[a]	Confining pressure (MPa)
1	3#	5266.94	0.08	2631.4	2.21	0
	4#	5276.36	0.10	2625.8	2.00	0
2	2#	5272.46	0.02	2621.2	1.82	5
	18#	5267.02	0.08	2569	0.21	5
3	8#	5282.35	0.21	2563.6	0.42	10
	5#	5250.79	0.39	2571.3	0.12	10
4	1#	5265.23	0.11	2527.1	1.84	20
	20#	5271.91	0.01	2523.1	1.99	20
5	9#	5292.7	0.41	2537.1	1.45	40
	15#	5267.08	0.08	2574.3	0.00	40

Where RE are relative errors, $\bar{x}$ is available value and is the means value of the variable x

[a] Relative errors of velocity and CT value are calculated by the following equation: RE = $\frac{(x-\bar{x})}{\bar{x}}$.

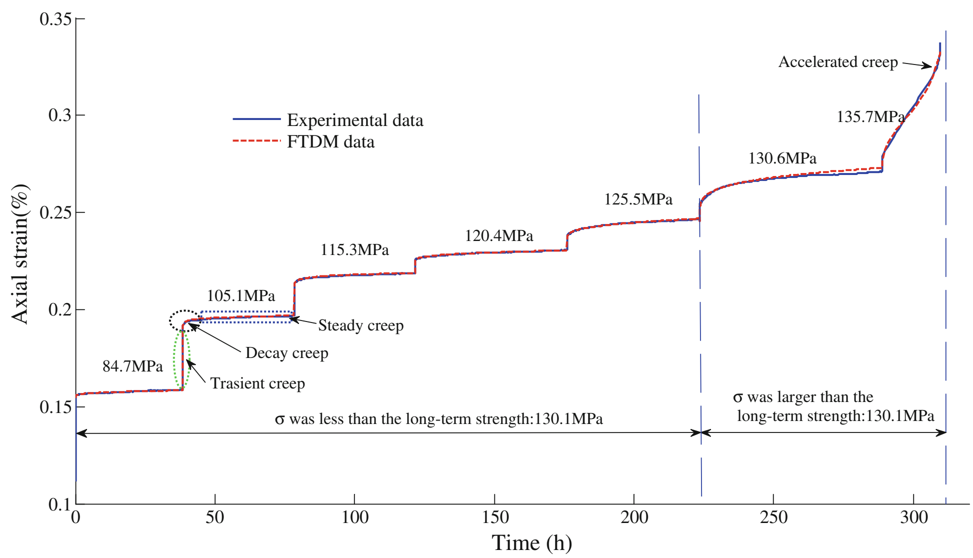

Fig. 5 Time-dependent strain curve and FTDM fitting result of marble under multi-stage uniaxial loading conditions (The long-term strength 130.1 MPa was identified using pattern search and least-square techniques (Chen et al. 2005) based on the experimental data)

2. When the constant load level was lower than approximately 80 % of the long-term rock strength, the creep rate of the marble under this load (i.e., 84.7 MPa) decayed instantaneously to a constant near-zero rate after loading stabilised (see Fig. 6a), while creep acceleration rapidly decreased to zero and remained constant (see Fig. 7). Attenuation creep occurred for a very short time and was not obvious, indicating that internal damage or microfractures could not continue to occur over time under a stable lower loading level. The rock sample's stress field instantly reached its equilibrium state and did not change over time.
3. When the constant load level was between 80 and 100 % of the rock's long-term strength, the creep rate and creep acceleration under this stable load gradually decreased and tended to become stable over time, with the creep rate close to zero and the creep acceleration equal to zero at the steady state (see Figs. 6a and 7). Under different constant loading conditions, the time for the creep rate to become stable increased with increasing stress levels, as shown in Fig. 8. These results indicated that microfractures had initiated and damage had begun to occur in weak local areas of the rock sample, causing increasing damage and time required for internal stress nonlinear adjustment to an equilibrium state with increased load. However, this load level was not sufficiently high to cause further microfractures in the rock sample and did not affect the rock's strength and stability; thus, the marble's yield strength did not change over time or become unstable.
4. When the constant load level exceeded the rock's long-term strength, the creep rate first decayed gradually and then became stable. Afterwards, it increased

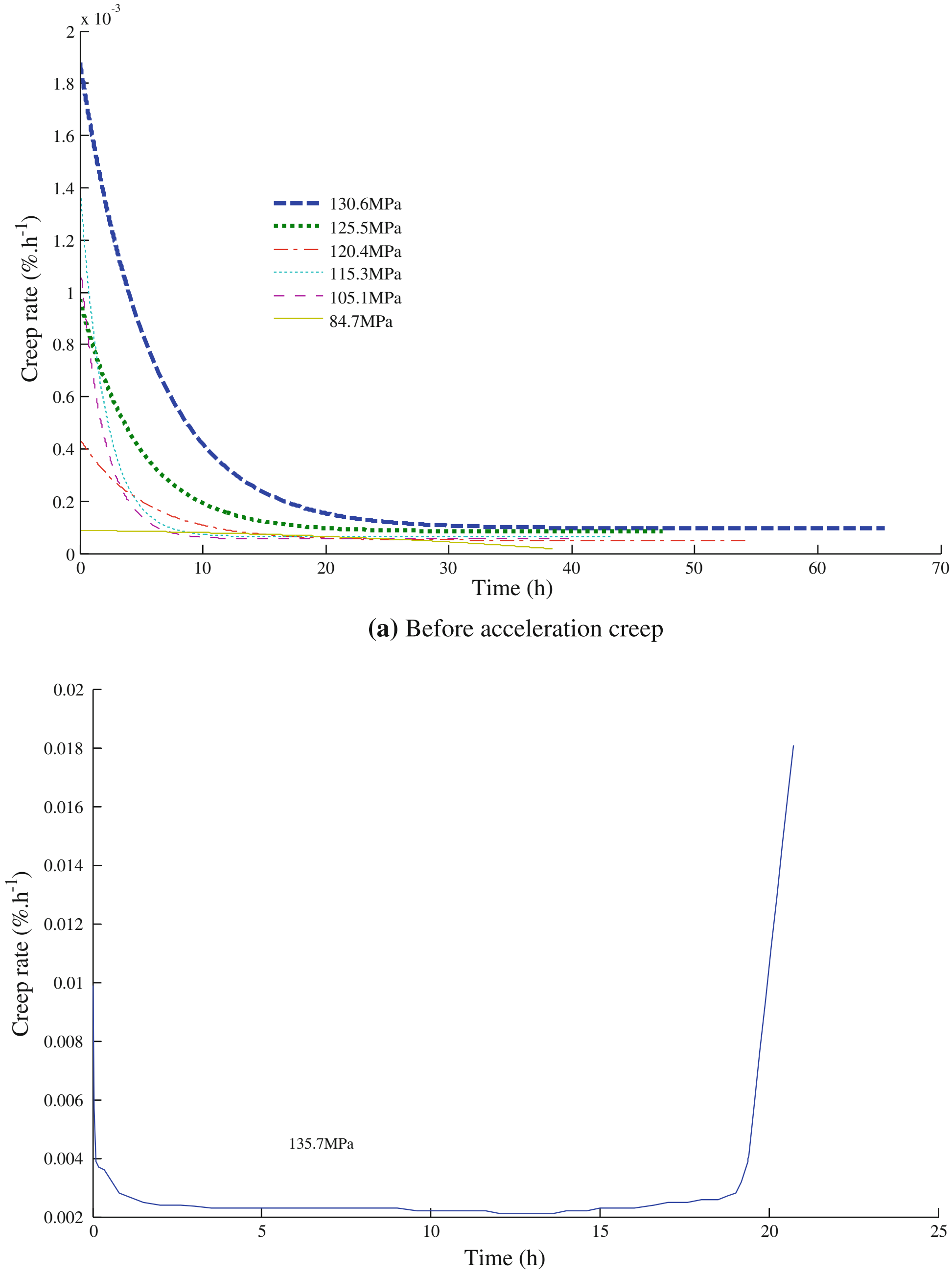

(a) Before acceleration creep

(b) At acceleration creep

Fig. 6 Axial creep rate evolution characteristics over time under different loading steps

rapidly until the rock sample was destroyed. Internal microfractures were initiated when the rock's external load was larger than its long-term strength, leading to its destruction. The duration of the steady creep depended on the stress level, the development of microfractures and the creep rate based on the stress level. When the cumulative damage within the rock samples could not support the current stress level, the samples generated accelerated creep and failure. The evolution of the creep rate over time is shown in Fig. 6b and the type of rock failure, mainly shear failure with scratches and debris on the failure surface, is shown in Fig. 9.

5. When the load was lower than the long-term strength, the steady creep rate increased slightly with an increase in stress level. When the load exceeded the long-term strength, the rock damage showed obvious characteristics and the steady-state creep rate increased rapidly with an increase in stress level, as shown in Fig. 8.

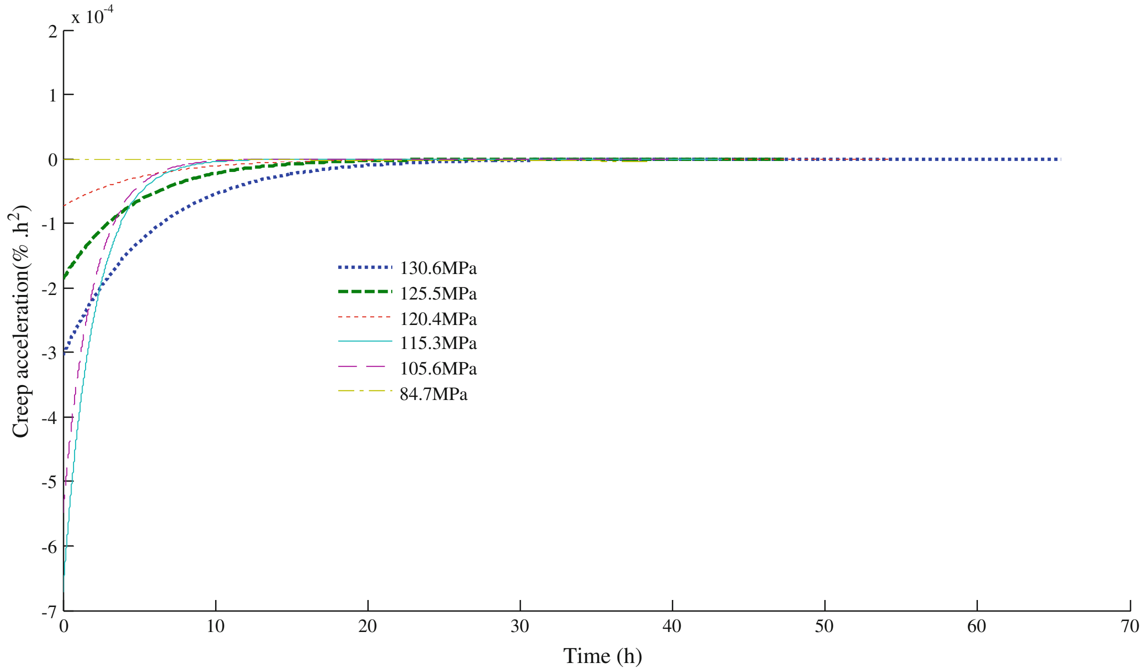

Fig. 7 Axial creep acceleration evolution characteristics over time under different loading steps

Fig. 8 Evolution law of axial steady creep rate and time interval from transient creep to steady creep under different loading steps

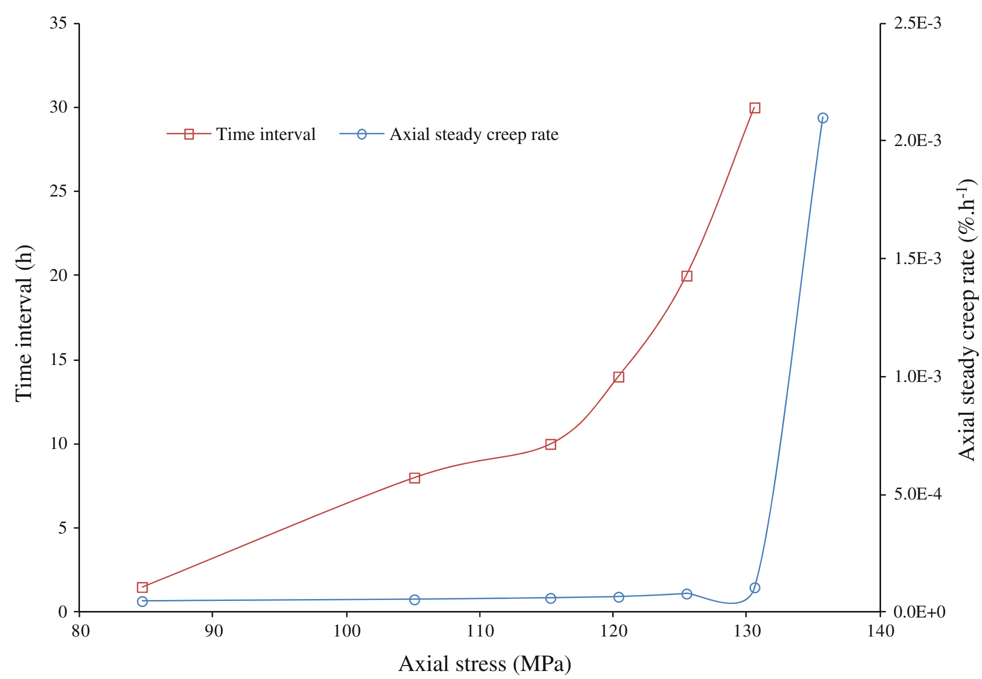

Time-dependent characteristics of the marble yield strength

Xu (1997) transformed the creep curve under multi-step loadings into a stress–strain curve under the same loading period. It was found that the yield strength of soft rock had an exponential relationship with time. Based on their ideas, the creep curve of marble under multi-step loadings was transformed into a stress–strain curve under the same loading period, as shown in Fig. 10. Figure 10 shows that every curve was made up of approximately linear and nonlinear segments with a significant turning point and that this point gradually became lower over time and approached a long-term strength limit. The marble showed a behaviourof mechanical properties from visco-elastic to visco-plastic, and its internal structure generated obvious

Fig. 9 Failure of marble under multi-step uniaxial compression creep testing

Fig. 10 Relationship between stress and strain at the same time under the same multi-step uniaxial compress creep test

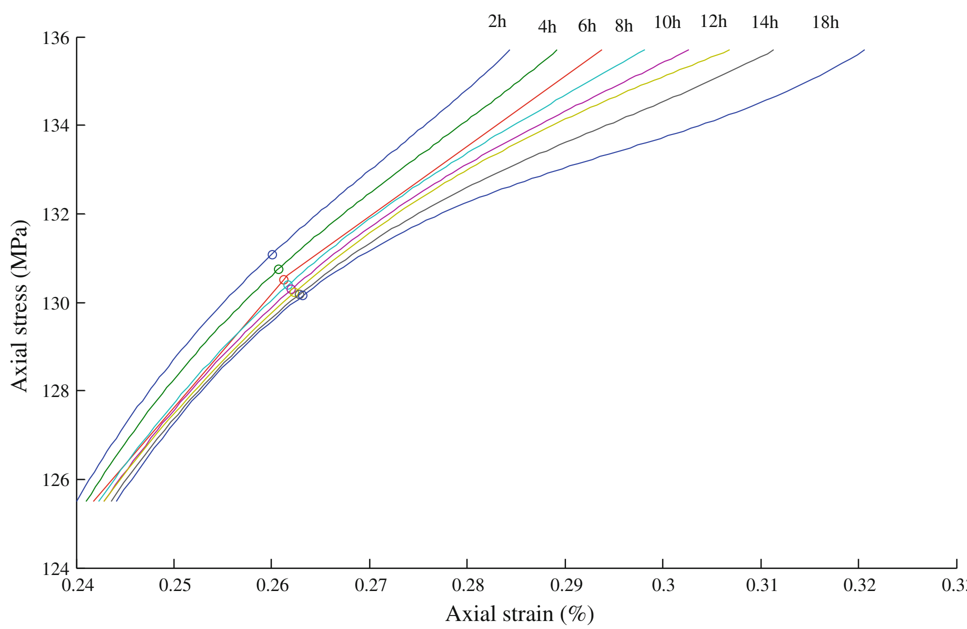

damage and deterioration and began to show a failure trend from this point forward. This point was named the yield point and the corresponding strength was its yield strength. The yield strength's relationship over time can be observed in Fig. 11 and described as follows:

$$\sigma_s = \begin{cases} \sigma_s^0 & \sigma \geq C \\ Ae^{-\alpha t} + c & \sigma > C \end{cases} \quad (1)$$

where σ is the rocks' long-term load, σ_s is the rock's yield strength, σ_s^0 is the rock's yield strength when rock damage initiates and has a magnitude equal to the yield strength obtained from conventional mechanical testing, A is a damage variable related to the rock's material properties, C is the rock's long-term yield strength that depends on the properties of the rock material itself, α is a parametric variable related to rock damage that is greater than zero and depends mainly on the rock's material properties and the external load level and t is the yield time when the rock begins to yield that is equal to the time when the rock began loading minus the time when the load is less than C.

When the external load $\sigma \leq C$, it is assumed that the rock is undamaged or has acquired only local weaknesses that do not influence its overall strength. In this case, the yield strength does not change with time but is always equal to σ_s^0 and the rock does not fail no matter how long the external load is applied. When the external load $\sigma > C$ damage is initiated in the rock then its yield strength attenuates as a negative exponential formation over time. When t is equal to zero, $\sigma_s = \sigma_s^0 = A + C$ and the yield strength is the same as the yield strength obtained from a conventional mechanical test. As $t \to \infty$, the rock's yield strength approaches its long-term strength, $\sigma_s = C$ and the attenuation speed of the rock's yield strength depends on the magnitude of α.

Fig. 11 Marble yield strength evolution law and fitting result over time when constant loading is higher than the material's long-term strength

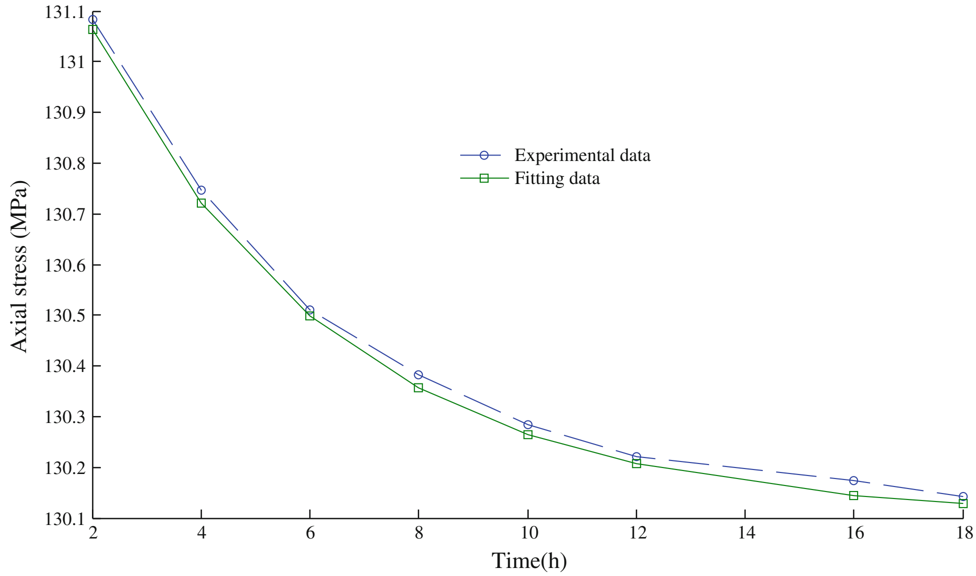

Time-dependent damage constitutive model of marble based on fractional order theory

Fractional order theory was introduced to analyse and describe damage characteristics and yield strength evolution law over time by considering the advantages of time-dependent constitutive models based on fractional calculus. The Riemann–Liouville fractional calculus theory (Nonnenmacher and Metzler 1995) was proposed for this study, for which the fractional integral of order β of the function $f(t)$ is defined as:

$$D^{-\beta}f(t) = \frac{1}{\Gamma(\beta)}\int_{0}^{t}(t-\tau)^{\beta-1}f(\tau)d\tau. \tag{2}$$

The fractional derivative is defined by:

$$D^{\beta}f(t) = \frac{d^n\left[D^{-(n-\beta)}f(t)\right]}{dt^n}, \tag{3}$$

where $D^{-\beta}$ and D^{β} are the Riemann–Liouville fractional integral operator and fractional derivative operator, respectively, $\beta \geq 0$ and $n-1 \leq \beta \leq n$, and n is the number of positive integers, $\Gamma(\beta)$ is the gamma function $\Gamma(\beta) = \int_0^\infty t^{\beta-1}e^{-t}dt$, $\mathrm{Re}(\beta) > 0$ and $\mathrm{Re}(\beta)$ is the real part of β. The gamma function has the following properties: $\Gamma(1+\beta) = \beta\Gamma(\beta)$, $\Gamma(1) = \Gamma(2) = 1$, $\Gamma\left(\frac{1}{2}\right) = \sqrt{\pi}$ and $\Gamma(-x) = \frac{-\pi\csc(\pi x)}{\Gamma(x+1)}$.

The viscous-damage component based on fractional calculus

An Abel body based on the fractional derivative (Kiryakova and Al-Sauabi 1999) was introduced to replace the Newton body in the model. The constitutive equation of the Abel body is:

$$\sigma(t) = \eta\, D^{\beta}[\varepsilon(t)] \tag{4}$$

where η is the coefficient of viscosity and β is the order of the fractional derivative, $0 \leq \beta \leq 1$. When $\beta = 0$, the Abel body is equal to spring body and can describe solid mechanical properties. When $\beta = 1$, the Abel body is equal to the Newton body and can describe fluid mechanical properties. Therefore, the Abel body can describe the mechanical properties of both solids and fluids.

When external load exceeds the long-term strength of the rock mass, the rock material will weaken with time and the yielding strength of the rock will also weaken with time. The weakening process can be described by the Abel body with a damage factor.

Based on the above test results, the damage to the Abel body can be described as follows:

$$\eta = \eta_0 e^{-\alpha t}, \tag{5}$$

where α is the damage coefficient related to the rock properties and external load and η_0 is the initial viscosity coefficient.

Combining Eqs. (4) and (5), the damage constitutive equation for the Abel body can be calculated as follows:

$$\sigma(t) = \eta_0 e^{-\alpha t}D^{\beta}[\varepsilon(t)] \quad 0 \leq \beta \leq 1. \tag{6}$$

Assuming $\sigma(t) = \sigma$ nd σ is a constant, the creep constitutive equation that considers the damage to the rock material is derived from Eq. (6) with a Laplace transform and inverse Laplace transform as follows:

$$\varepsilon(t) = \frac{\sigma}{\eta_0^{\beta}}t^{\beta}\sum_{k=0}^{\infty}\frac{(\alpha t)^k}{\Gamma(k+1+\beta)}, \tag{7}$$

where k is a non-negative integer and the other parameters are as described above.

Assuming $\varepsilon(t) = \varepsilon$ and ε is a constant, the relaxation equation in Eq. (8) can be obtained from Eq. (6) with a Laplace transform and inverse Laplace transform:

$$\sigma(t) = \frac{\varepsilon \eta_0 e^{-\alpha t}}{\Gamma(1-\beta) t^{\beta}}, \tag{8}$$

where the parameters are as described above.

FTDM

An improved fractional-order time-dependent damage model (FTDM) was proposed to accurately describe the properties of the marble during the instantaneous creep, decay creep, steady creep and accelerating creep stages and to explain the evolution law of the damage characteristics and the rock's yield strength over time in the early stages of accelerating creep. The Hoke body, improved A/H body and new A/S body are in series in this model, as shown in Fig. 12. The A/H body consists of an Abel body parallel to a Hoke body and the A/S body is built with a Saint–Venant body parallel to an Abel body. The Hoke body is used to express the instantaneous creep property of the marble, the improved A/H body is utilized to describe the mechanical properties of the marble during the decay creep and steady creep and the new A/S body is introduced to explain the evolution law of the damage characteristics and the rock's yield strength over time in the early stages of accelerating creep.

When $\sigma \leq C$, the damage does not increases over time in the rock, no slip occurs in the S body and the A/S body can be treated as a rigid body. FTDM is a new generalised Kelvin model, in which the Newton body is replaced by the Abel body for accurately describing the properties of the marble during the decay creep and steady creep. Its equation can be written as follows:

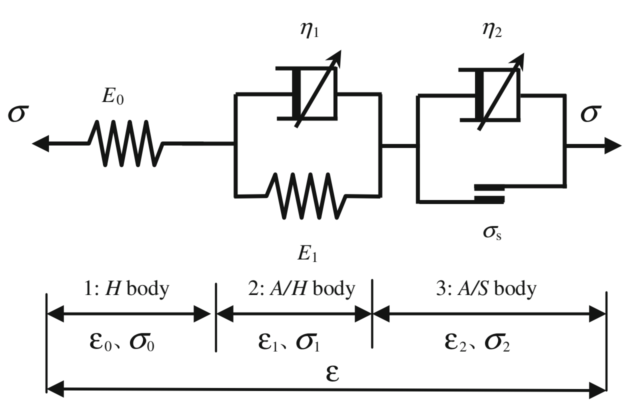

Fig. 12 Fractional-order time-dependent damage model (FTDM)

$$\begin{cases} \sigma_0 = E_0 \varepsilon_0 \\ \sigma_1 = E_1 \varepsilon_1(t) + \eta_1 D^{\beta}[\varepsilon_1(t)] \\ \sigma_0 = \sigma_1 = \sigma \\ \varepsilon = \varepsilon_0 + \varepsilon_1 \end{cases}, \tag{9}$$

where σ is the external load; σ_0 and σ_1 are loads on the elastic body and A/H body, respectively; ε, ε_0 and ε_1 are the total strain, elastic body strain and A/H body strain, respectively; E_0 and E_1 are the elastic moduli of the elastic body and A/H body, respectively; η_1 is the viscosity coefficient of the Abel body; and β is the order of the fractional derivative, with $0 \leq \beta \leq 1$.

Given the external load σ as a constant, the creep constitutive equation can be solved using Eq. (9) as follows:

$$\varepsilon(t) = \frac{\sigma}{E_0} + \frac{\sigma}{\eta_1} \sum_{k'=0}^{\infty} \left(-\frac{E_1}{\eta_1}\right)^{k'} \frac{t^{\beta(k'+1)}}{\Gamma(\beta k' + \beta + 1)}, \tag{10}$$

where k' is a non-negative integer and the other parameters are as described above.

Assuming strain ε is a constant, the relaxation constitutive relationship shown in Eq. (11) can be obtained from Eq. (9):

$$\sigma(t) = \varepsilon_0 \frac{E_0 E_1}{E_0 + E_1} \sum_{K=0}^{\infty} \left(-\frac{E_0 + E_1}{\eta_1}\right)^{k+1} \frac{t^{k\beta+1}}{\Gamma(1+\beta+k\beta)} + \varepsilon_0 E_0 \sum_{K=0}^{\infty} \left(-\frac{E_0 + E_1}{\eta_1}\right)^{k+1} \frac{t^{k\beta}}{\Gamma(1+k\beta)}. \tag{11}$$

When the external loading $\sigma > C$, damage to the rock material is initiated, its yield strength begins to decrease over time, the S body begins to slip and the Abel body parallel to the S body begins to flow under the load $\sigma - \sigma_s$. The equations of FTDM are described in Eq. (12):

$$\begin{cases} \sigma_0 = E_0 \varepsilon_0 \\ \sigma_1 = E_1 \varepsilon(t) + \eta_1 D^{\beta}[\varepsilon_1(t)] \\ \sigma_2 = \sigma_s + \eta_2 D^{\beta}[\varepsilon_2(t)] \\ \sigma_0 = \sigma_1 = \sigma_2 = \sigma \\ \varepsilon = \varepsilon_0 + \varepsilon_1 + \varepsilon_2 \end{cases}, \tag{12}$$

where σ is the external load; σ_0, σ_1 and σ_2 are the loads on the elastic body, A/H body and A/S body, respectively; ε_2 is the strain of the A/S body; η_2, equal to η_0, $e^{-\alpha t}$, is the viscosity coefficient of the Abel body considering the rock's damage characteristics in which η_0 is the initial viscosity coefficient and α is the damage variable; σ_s is the rock's yield strength that incorporates the damage to the rock described by Eq. (1); and the other parameters are as described above.

Assuming the external load σ is constant, the creep equation can be obtained by solving Eq. (12):

$$\varepsilon(t) = \frac{\sigma}{E_0} + \frac{\sigma}{\eta_1}\sum_{k'=0}^{\infty}\left(-\frac{E_1}{\eta_1}\right)^{k'}\frac{t^{\beta(k'+1)}}{\Gamma(1+\beta+\beta k')} + \frac{\sigma - C}{\eta_0}t^{\beta}\sum_{k=0}^{\infty}\frac{(\alpha t)^k}{\Gamma(1+k+\beta)} - \frac{A}{\eta_0}\frac{t^{\beta}}{\Gamma(1+\beta)}, \tag{13}$$

where k and k' are non-negative integers, A is the damage variable related to the rock properties, C is the long-term strength of the rock, α is the damage variable and the other parameters are as described above.

Verification of FTDM

The feasibility and applicability of FTDM were verified with typical time-dependent experimental tests on the marble.

Determination of the time-dependent yield strength of marble

It has always been challenging to determine the stress threshold of the plastic flow initiated by mechanic testing in the laboratory under external long-term loading.

Researchers proposed different methods of determining the stress threshold based on their research objectives. For example, Xu (2005) obtained the stress value by a series of rheological experiments, while Zhou (1990) proposed that the stress threshold of the initiated plastic flow is the stress value when the incremental Poisson's ratio reaches 0.5. Zhao (2008) assumed that the stress when plastic flow occurred was equal to 0.7–0.8 of the uniaxial strength. These results were acquired under the assumption that the rock's yield strength was constant. In fact, internal damage was initiated when the external load exceeded the rock's long-term strength and its yield strength began to change over time. Therefore, it is reasonable to determine a rock's yield strength by fitting parameters into Eq. (1) according to the experimental data, knowing that the yield strength law changes further over time. The parameters in Eq. (1) are identified using pattern search and least-square techniques improved by the Levenberg–Marquardt algorithm (Chen et al. 2005) based on the experimental data and represented in Eq. (14) and the fitting results are shown in Fig. 11.

$$\sigma_s = \begin{cases} 131.6\,\text{MPa} & \sigma \leq 130.1\,\text{MPa} \\ 1.5e^{-0.2205t} - 130.1\,\text{MPa} & \sigma > 130.1\,\text{MPa} \end{cases} \tag{14}$$

Parameter identification process for FTDM

The parameters of FTDM were determined using the back analysis method, in which the least squares method is used with the following identification process.

Table 2 Rock creep parameters of FTDM under different loads when $\sigma \leq 130.1$ MPa

Loads (MPa)	E_0 (GPa)	E_1 (GPa)	η_1 (GPa·h)	k'	β
84.7	55	152	5,691	9	0.23
105.1	64	320	355	9	0.03
115.3	59	400	661	9	0.05
120.4	54	70	5,833	9	0.26
125.5	53	31	4,650	9	0.32

First, N pairs of experimental data are collected in the form of (t_n, ε_n) $n = 1, 2, 3, \ldots, N$.

Next, an evaluation function is established to evaluate the results of the back analysis as follows:

$$Q = \sum_{n=1}^{N}[\varepsilon_n - f(t_n, b)]^2 \tag{15}$$

where b is a vector composed of the parameters to be identified, (t_n, ε_n) is the nth pair of experimental data t_n is the time at which the No. n data are recorded, ε_n is the strain corresponding to time t_n, f is the corresponding time-dependent damage constitutive model and $n = 1, 2, \ldots\ldots, N$.

Then, pattern search and least-square techniques improved by the Levenberg–Marquardt algorithm (Chen et al. 2005) are introduced and the tolerance and initial values of the parameters to be identified are set.

Finally, the parameters are identified. If an error meets the tolerance, the parameter identification is over. Otherwise, the parameters are improved further until the proper parameters are recognised.

Verification of FTDM

When $\sigma > 130.1$ MPa, it was assumed that no damage occurred in the marble. The main mechanical characteristics include transient creep, decay creep and steady creep; thus, the time-dependent mechanical properties can be described by Eq. (10). The main parameters to be determined include E_0, η_1, k' and β. The results from using the method introduced above are shown in Table 2 and the fitting results are shown in Fig. 5. It can be concluded that the transient creep, decay creep and steady creep properties of the rock were well described by the model proposed in this study.

When $\sigma > 130.1$ MPa, damage started to initiate inside the marble. The main mechanical characteristics include transient creep, decay creep and non-steady creep when the load was larger than the rock's long-term strength. Therefore, the time-dependent mechanical properties were described by Eq. (13). The main parameters to be determined included A, α C, E_0, E_1, η_1, k, k and β. The

Table 3 Rock creep parameters of FTDM under different loads when $\sigma > 130.1$ MPa

Loads (MPa)	E_0 (GPa)	E_1 (GPa)	η_1 (GPa·h)	η_0 (GPa·h)	k'	k	β
130.6	51.7	298	3,544	4,959	1	7	0.55
135.7	49.3	73.6	2,552	7,567	1	7	0.67

Table 4 Rheological parameters of the Burgers model

Loads (MPa)	E_0 (GPa)	E_1 (GPa)	η_1 (GPa.h)	η_2 (GPa.h)
125.5	53	2,610	10,7300	1,961
135.7	49	2,130	5,860	4,940

parameters related to the marble's yield strength, A, α and C, were determined in the last section with values of 1.5 MPa, 0.2205 h^{-1} and 130.1 MPa, respectively. Other parameters were determined with the method introduced above, with the results shown in Table 3 and the fitting results shown in Fig. 5. It can be concluded that the time-dependent damage properties and accelerated creep stage of marble were described properly by this proposed model.

Fractional-order time-dependent damage model, which considered changes in the marble's yield strength over time, accurately described the rock's transient creep, decay creep, steady creep and accelerated creep and was found suitable for rock engineering needs.

Comparison analysis with other models

The proposed model was compared with the Burgers model assuming $\sigma > 130.1$ MPa and $\sigma > 130.1$ MPa.

When $\sigma \leq 130.1$ Pa, creep testing at $\sigma = 25.5$ MPa was taken as a typical example. The parameters of the two models were recognised by the method introduced above and the results are shown in Tables 2 and 4. Comparisons with the experimental data are shown in Fig. 13. It was clear that FTDM better described the creep properties of marble than the Burgers model, regardless of the steady creep or decay creep stage.

When $\sigma > 130.1$ Pa, creep testing at $\sigma = 135.7$ MPa was taken as a typical example. The parameters of the two models were again recognised by the method introduced above and the results are shown in Tables 2 and 4. Comparisons with the experimental data are shown in Fig. 14.

It was concluded that the Burgers model did not properly describe the characteristics of the accelerated creep because it only increased the rate of creep as steady creep rate, and the FTDM better described the properties of the acceleration creep when considering the marble's time-dependent damage properties and attenuation characteristics under long-term loading.

Sensitivity analysis of the FTDM parameters

A sensitivity analysis was performed based on the creep testing example at $\sigma = 135.7$ MPa.

Sensitivity analysis of the ratio of terms of series ξ

Equation (13) contains a term of series that which should be addressed when the calculation is performed, and it was found that the ratio of the breaking terms of two series had a major influence on the proposed model and especially on the accelerating deformation stage.

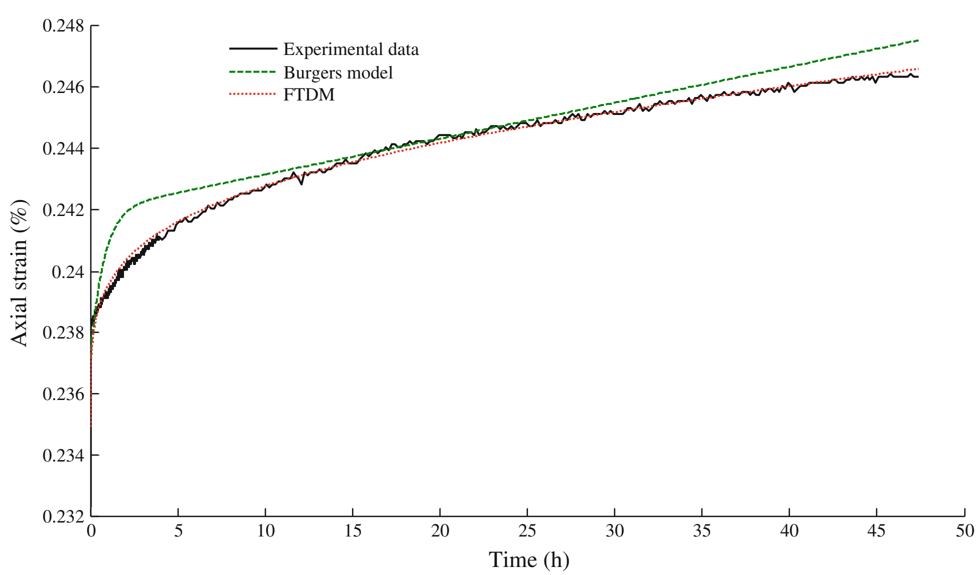

Fig. 13 Comparison of FTDM, Burgers model and experimental data at the $\sigma = 125.5$ MPa loading step

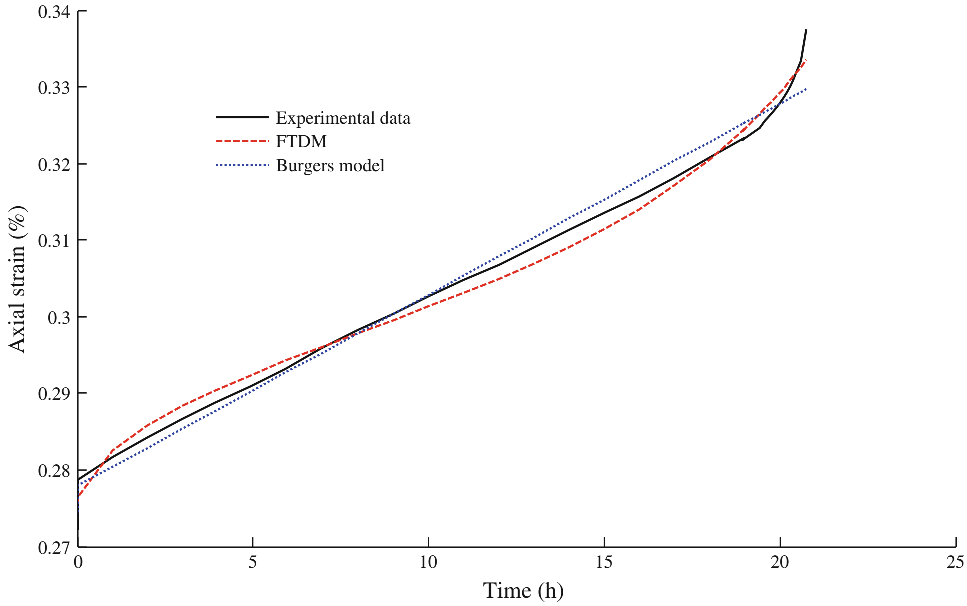

Fig. 14 Comparison of FTDM, Burgers model and experimental data at the $\sigma = 135.7$ MPa loading step

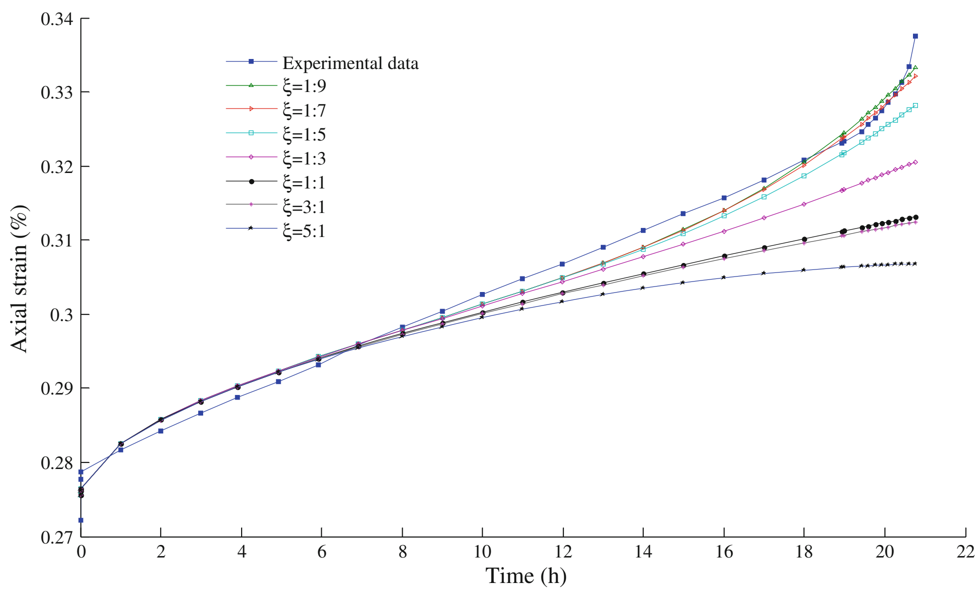

Fig. 15 Influence of ξ on FDTM accelerating creep at $\sigma = 135.7$ MPa loading step

Assume ξ is the ratio of the breaking terms of the two series and let:

$$\xi = \frac{k'}{k}(k' \geq 1, \quad k \geq 1), \tag{16}$$

where k' is the term broken by the first series and k is the term broken by the second series in Eq. (13).

The relevant parameters were taken as the following: $E_0 = 49.3$ GPa, $E_1 = 73.6$ GPa, $\eta_1 = 2.6$ GPa, $\eta_0 = 7.6$ GPa, $\beta = 0.54$, $A = 1.5$ MPa, $\alpha = 0.2205$ h-1 and $C = 130.1$ MPa. By keeping these parameters constant and letting the value of ξ decrease gradually, conclusions were drawn from Fig. 15 as follows.

1. ξ was smaller, the attenuation creep time was shorter and the accelerating creep was more obvious.
2. ξ had poor sensitivity at the initial stage of attenuation creep and different ξ values had little influence on the fitting results of Eq. (13).
3. ξ was smaller and the creep rate was larger during the steady creep stage.

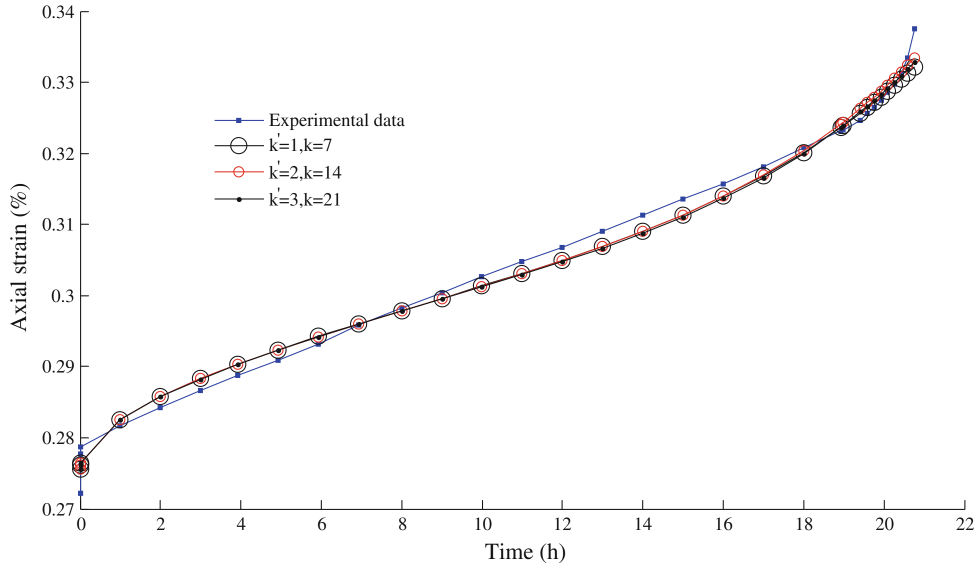

Fig. 16 Influence of k' and k on FTDM accelerating creep with constant ξ at $\sigma = 135.7$ MPa loading step

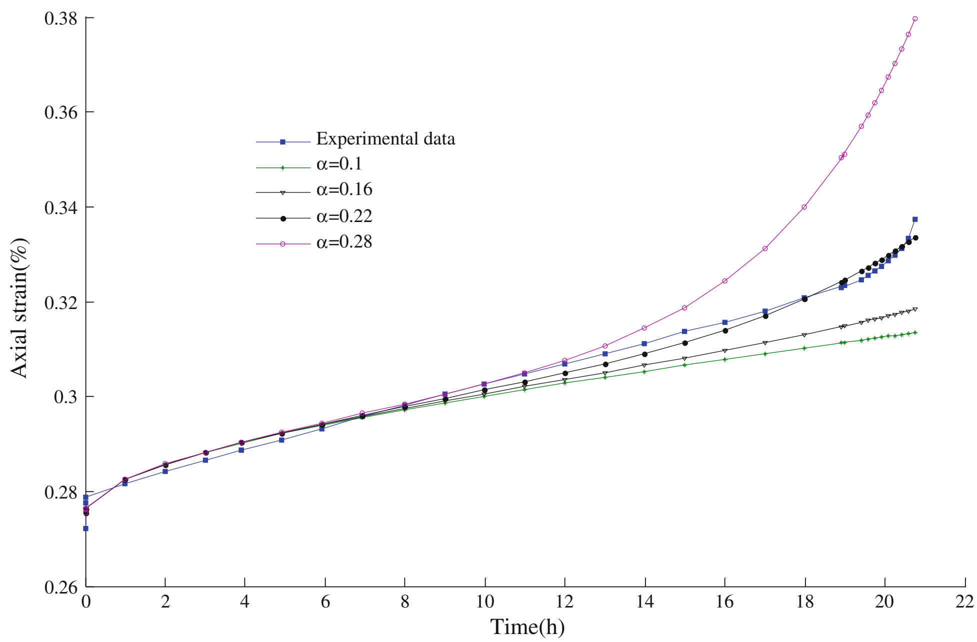

Fig. 17 Comparison of calculated and test results with varying damage parameter α at $\sigma = 135.7$ MPa loading step

Based on the Jinping's marble mechanical behaviour at the accelerating creep stage, the ratio of breaking terms of the two series was taken as 1:7. The results showed that this ratio was reasonable.

Figure 16 shows that the fitting result was unaffected when the ratio of 1:7 was kept constant and the values of k' and k were changed.

Sensitivity analysis of the damage parameters α

k' and k were taken as 1 and 7, respectively, and the other FTDM parameters were the same as the section mentioned above, while αas gradually increased from 0.1. Figure 17 described the transient creep, decay creep and steady creep, but it was difficult to depict accelerating creep when αas was small using Eq. (13). Increasing α rapidly enhanced the ability of Eq. (13) to describe accelerating creep, but a good α value must be determined by engineering or experimental results.

The results of increasing α were assessed according to Eq. (15). Figure 18 indicates the existence of an optimal α value that minimises the residual sum of the square of the strain monitored and strain calculated. Assuming that the optimal value is α_0, the residual sum of the square slowly decreases nonlinearly with an increase in α when $\alpha < \alpha_0$ and the residual sum of the square increases rapidly and the gradient increases dramatically with an increase in α when $\alpha > \alpha_0$. When $\alpha > \alpha_0$, α is very sensitive. Therefore, it is necessary to optimise the value of α. Based on the optimisation results, the fitting results of the time-dependent damage constitutive model are good when α is 0.22.

Sensitivity analysis of β

Parameters k' and k and α were taken as 1, 7 and 0.22, respectively, and the other model parameters were the same as in the section mentioned above. β was increased gradually and Fig. 19 shows that the steady creep rate is higher and the increasing rate of creep at the accelerating stage was faster when β was larger. This result indicates the importance of selecting an appropriate number of fractional orders to describe the time-dependent damage characteristics of the marble, especially at the accelerating stage.

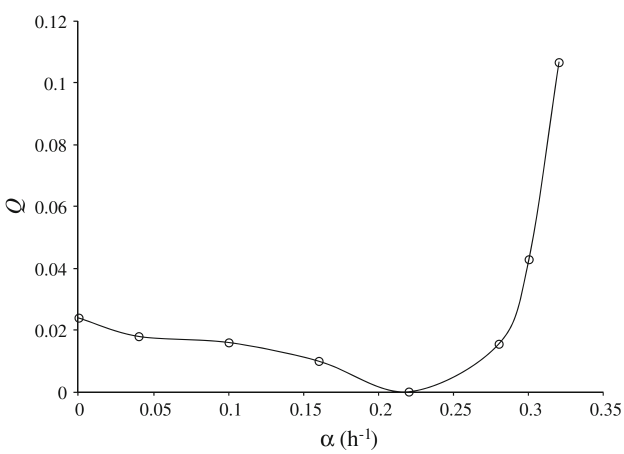

Fig. 18 Effect of the damage parameter α on FTDM accelerating creep at $\sigma = 135.7$ MPa loading step

When β was changed from a small to a large value, the results were assessed with Eq. (15). Figure 20 shows that the residual sum of the square of the strain monitored and strain calculated decreased and then increased with an increase in β, and that an optimal β value existed that minimised the residual sum of the square of the experimental data and the calculated value. Therefore, it is necessary to optimise the value of β when the model is used to describe the mechanical properties of the rock. The fitting results of the time-dependent damage constitutive model are most appropriate when β is equal to 0.57.

Discussion

Although some interesting time-dependent investigations on marble have been implemented and some interesting results were obtained in this paper, some questions need to be discussed and many further studies need to be carried out:

1. The yield strength's negative exponential attenuation law over time for the marble was obtained based mainly on laboratory test results. The test durations were relatively short, with most ranging from 15 to 40 days. Whether these results can be used in future rock engineering remains to be decided and will require more study of this topic.
2. A time-dependent damage constitutive model for the marble was built based on fractional calculus theory and damage variables; however, only one dimensional constitutive equations were derived and verified based on uniaxial creep data. What are the three dimensional

Fig. 19 Creep curve at different β values and $\sigma = 135.7$ MPa loading step

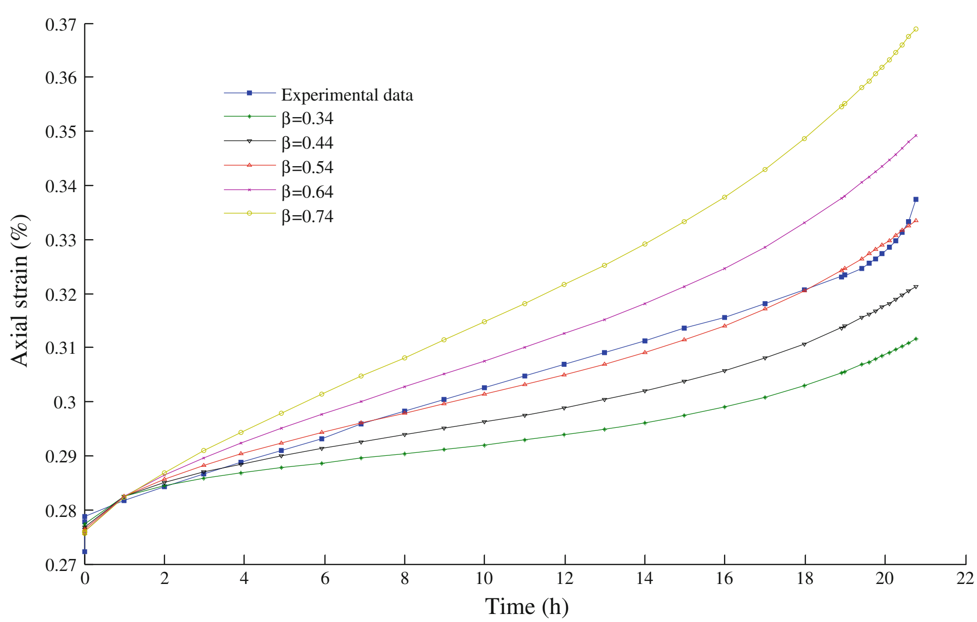

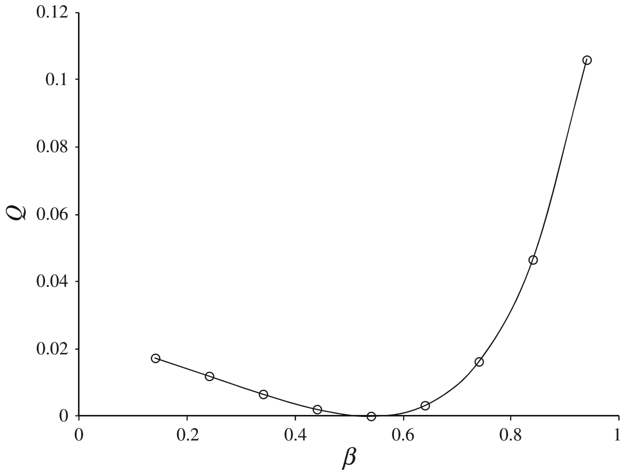

Fig. 20 Effect of fractional order β on FTDM accelerating creep at $\sigma = 135.7$ MPa loading step

constitutive equations? It needs to be extended and certified further.

3. The damage characteristic of the marble was observed in laboratory tests when the constant load level was between 80 and 100 % of the rock's long-term strength; however, the proposed model only can describe damage characteristic of the marble during the early acceleration creep stage. It is necessary to introduce a new variable for describing an initiated damage characteristic as the constant load level was between 80 and 100 % of the rock's long-term strength.
4. In this paper, the time-dependent damage characteristic of the marble was described based on creep state and the deformation characteristic of rock samples. It is better for describing the time-dependent damage characteristic quantificationally that if acoustic emission monitoring can be implemented during creep testing. The relation between crack density and acoustic emission events can be found.
5. The time-dependent damage relaxation equations were derived, while relaxation characteristics on the marble have not been verified by tests.
6. Although model was obtained under multi-step loading, the model can be used to do a single creep test. The parameter of Eq. (1) cannot be identified by the fitting method mentioned above under the single creep test, while they can be recognized by another method $\alpha_s^{0,}$ which is the conventional yield strength of rock material. It can be obtained directly by conventional mechanical testing, C can be got by simple creep test (Xu 2005; Zhou 1990), A can be calculated by Eq. (1) when t is equal to zero and α can be evaluated between 0 and 1 as a rule of thumb.

Conclusion

The following conclusions can be drawn from this study:

1. Field observations and laboratory tests on marble from the Jinping II hydropower station gave the following results. (a) When the constant load was below 80 % of the rock's long-term strength, the marble sustained almost no damage and the yield strength was time-independent. (b) When the constant load was between 80 and 100 % of the rock's long-term strength, damage was initiated in the marble's local weak areas. A larger constant load resulted in more damage to the rock and a longer time period for nonlinear adjustment of the internal stress equilibrium in the marble. However, the damage caused by this load was still insufficient to threaten the integral strength and stability of the rock. Thus, the yield strength of the marble was still constant over time. (c) When the constant load was above the rock's long-term strength, the damage was initiated completely inside the rock. The duration of steady creep was dependent on the stress level and the degree and developing rate of damage. Accelerated creep and failure occurred when the accumulated damage kept building and the rock could not tolerate the stress level. The marble's yield strength showed negative exponential attenuation over time.
2. Considering the damage and time-dependent characteristics of the rock's yield strength, a time-dependent damage constitutive model for the marble was built based on fractional calculus theory and damage variables. Comparisons with test results and other models showed that the model accurately described not only decay creep and stability creep but also the acceleration creep of the marble. Moreover, the model described the time-dependent characteristics for the marble's yield strength with negative exponential attenuation over time when the constant load was above the rock's long-term strength.
3. A sensitivity analysis was performed on parameters related to the time-dependent damage characteristics of the proposed model. The results showed that parameters ξ, α and β had a relatively large influence on the model's time-dependent characteristics. The proposed model best described the acceleration creep and time-dependent characteristics when $\xi = 1.7$, $\alpha = 0.22$ and $\beta = 0.57$.

Acknowledgments Financial support from the National Natural Science Foundation of China under Grant No. 50909092, the Special Funds for Major State Basic Research Project under Grant No. 2010CB732006, the support of K.C. Wong Education Foundation, Hongkong and the Program for New Century Excellent Talents in University under Grant No. NCET-08-0662 are gratefully acknowledged. The authors would like to thank Gao H. and Liu J. G. for their help in the lab.

References

Bagley RL, Torvik PJ (1983) A theoretical basis for the application of fractional calculus to viscoelasticity. J Theol 27(3):201–210

Beda T, Chevalier Y (2004) New methods for identifying rheological parameter for fractional derivative modeling of viscoelastic behavior. Mech Time-Depend Mater 8:105–118

Chen J (2013) Time-dependent deformation and fracture mechanisms of hard rock and engineering behavioural analysis. Doctor dissertation. Institute of Rock and Soil Mechanics, Chinese Academy of Science,Wuhan

Chen BR, Feng XT (2008) Universal viscoelastic combination model and its engineering applications. Chin J Rock Mech Eng 27(5):1028–1035

Chen BR, Feng XT et al (2005) Rheological model and parameters identification of rock based on pattern search and least-square techniques. Chin J Rock Mech Eng 24(2):207–211

Deng R (2001) A new rheological model for rocks. Chin J Rock Mech Eng 20(6):780–784

Feng XT, Zhou H (2006) Research report on stability of surrounding rock mass and structure design of headrace tunnels of Jinping II hydropower station at Yalong River during invite public bidding and design phase. Institute of Rock and Soil Mechanics, the Chinese Academy of Science, Wuhan

Jin J, Cristescu ND (1998) An elastic/viscoplastic model for transient creep of rock salt. Int J Plasticity 14:85–107

Kiryakova V, Al-Sauabi B (1999) Explicit solutions to Hyper-Bessel integral equations of second kind. Comput Math Appl 37:75–86

Koeller RC (1984) Application of fractional calculus to the theory of viscoelasticity. ASME J Appl Mech 51:299–307

Molladavoodi H, Mortazavi A (2011) A damage-based numerical analysis of brittle rocks failure mechanism. Finite Elem Anal Des 47:991–1003

Nonnenmacher TF, Metzler R (1995) On the Riemann-Liouville fractional calculus and some recent applications. Fractals 3(3):557–566

Professional Standards Compilation Group of People's Republic of China (2007) Code for rock tests of hydroelectric and water conservancy engineering. China Electric Power Press, Beijing

Song DY, Jiang TQ (1998) Study on the constitutive equation with fractional derivative for viscoelastic fluids: modified Jeffreys model and its application. Rhelo Acta 37:512–517

Wang GJ (2004) A new constitutive creep-damage model for salt rock and its characteristics. Int J Rock Mech Min Sci 41(Supp. 1):61–73

Welch SWJ, Rorrer RAL, Duren RG (1999) Application of time-based fractional calculus methods to viscoelastic creep and stress relaxation of materials. Mech Time-Depend Mater 3:279–303

Xie N (2011) A micromechanics-based elastoplastic damage model for quasi-brittle rocks. Comput Geotech 38:970–977

Xu HF (1997) Time dependent behaviours of strength and elasticity modulus of weak rock. Chin J Rock Mech Eng 16(3):246–251

Xu WY (2005) Investigation on triaxial rheological mechanical properties of greenschist specimen (II): model analysis. Rock Soil Mech 25(5):693–698

You M (2007) Discussion on "Nonlinear viscoelasto-plastic rheological model (Hohai model) of rock and its engineering application". Chin J Rock Mech Eng 26(3):637–640

Zhao Y (2008) Elastovisco-plastic rheological experiment and nonlinear rheological model of rocks. Chin J Rock Mech Eng 27(3):477–486

Zhou W (1990) Advanced rock mechanics. China Water Power Press, Beijing

Zhou H (2011) A creep constitutive model for salt rock based on fractional derivatives. Int J Rock Mech Min Sci 48:116–121